Chinese Chemical Letters 35 (2024) 109549

Contents lists available at ScienceDirect

Chinese Chemical Letters

journal homepage: www.elsevier.com/locate/cclet

Constructing thermoresponsive PNIPAM-based microcarriers for cell culture and enzyme-free cell harvesting

Yunan Yuan[a,b,d], Zhimin Luo[c,e], Jie Chen[a,d], Chaoliang He[a,b], Kai Hao[c,*], Huayu Tian[a,b,c,d,e,*]

[a] CAS Key Laboratory of Polymer Ecomaterials, Changchun Institute of Applied Chemistry, Chinese Academy of Sciences, Changchun 130022, China
[b] School of Applied Chemistry and Engineering, University of Science and Technology of China, Hefei 230026, China
[c] College of Chemistry and Chemical Engineering, Xiamen University, Xiamen 361005, China
[d] Jilin Biomedical Polymers Engineering Laboratory, Changchun 130022, China
[e] Innovation Laboratory for Sciences and Technologies of Energy Materials of Fujian Province (IKKEM), Xiamen 361005, China

ARTICLE INFO

Article history:
Received 14 November 2023
Revised 17 January 2024
Accepted 19 January 2024
Available online 23 January 2024

Keywords:
Microcarrier
Temperature-responese
PNIPAM
Polymers
Cell culture

ABSTRACT

The development of large-scale cell cultivation and non-invasive cell harvesting is highly desired in various fields, including biological regeneration and pharmaceutical research. When using traditional microcarriers for cell culture, trypsinization is often necessary during cell collection, leading to partial cells damage. In this work, we developed a thermoresponsive glass microcarrier modified with poly(γ-propargyl-L-glutamate) (PPLG) and poly(*N*-isopropylacrylamide) (PNIPAM). We utilized these microcarriers for three-dimensional cell culture and enzyme-free cell harvesting, and the results indicated that the prepared microcarriers exhibited excellent non-invasive cell culture performance.

With the continuous advancement of biotechnology, there is a growing emphasis on rapidly obtaining a large number of cells for various applications, such as regenerative medicine, tissue-engineering and pharmaceutical research. In comparison to traditional two-dimensional (2D) cell culture, the utilization of microcarriers for three-dimensional (3D) cell culture has emerged as a straightforward method to achieve large-scale cell production [1,2]. Microcarriers are spherical particles ranging in size range of 100–300 μm with a higher specific surface area-to-volume ratio to promote cell growth and enhance cell densities [3,4]. Today, a wide variety of microcarriers, including those made from dextran, glass, collagen, polystyrene, polyethylene and chitosan have been developed [5]. However, most current commercial microcarriers, including Cytodex-3, fail to preserve the integrity of surface proteins on harvested cells. This is primarily due to the conventional method of cell harvesting from microcarriers, which relies on enzymes that can damage cells and extracellular matrix (ECM) proteins [6]. Therefore, there is a strong need to develop an efficient microcarrier that can enable large-scale cultivation and noninvasive cells harvesting.

Poly(*N*-isopropylacrylamide) (PNIPAM) is one of smart temperature-sensitive polymers with a hydrophilic amide group (-CONH-) and a hydrophobic isopropyl group [-CH(CH_3)$_2$-] along its molecular chain, which leads to a lower critical solution temperature (LCST) of approximately 32 °C [7,8]. Grafting PNIPAM onto the surfaces of microcarriers is a promising strategy for creating thermoresponsive surfaces to enable non-invasive cell harvest. By grafting PNIPAM onto the surface of microcarriers, cell attachment and detachment can be easily controlled by adjusting the external temperature. At 37 °C, PNIPAM-grafted surfaces become hydrophobic and adopts a globular conformation, facilitating protein absorption and cell attachment. Below the LCST, PNIPAM turns hydrophilic and random coil, promoting cell detachment without causing damage to the cell body and underlying extracellular matrix (ECM) proteins [9,10]. Teruo Okano [11] grafted P(IPAAm-*co*-APTAC-*co*-*t*BAAm) terpolymer onto the microcarriers surfaces. Under low-temperature conditions, nearly all cells detached from the thermoresponsive bead surfaces within 120 min.

In this study, we have developed a thermoresponsive microcarrier modified with biocompatible poly(γ-propargyl-L-glutamate) (PPLG) and PNIPAM. Leveraging the temperature-dependent of hydrophilicity and hydrophobicity transition properties of PNIPAM, these prepared thermoresponsive microcarriers facilitate controlled and noninvasive cell collection while enhancing cell production in a 3D culture setting (Fig. 1a). Initially, we synthesized amino-modified glass microspheres upon functionalization with APTES, followed by grafting PPLG *via* surface amnio-initiated *N*-carboxyanhdyride (NCA) ring-opening polymerization.

* Corresponding authors.
E-mail addresses: kaihao@ciac.ac.cn (K. Hao), thy@xmu.edu.cn (H. Tian).

https://doi.org/10.1016/j.cclet.2024.109549
1001-8417/

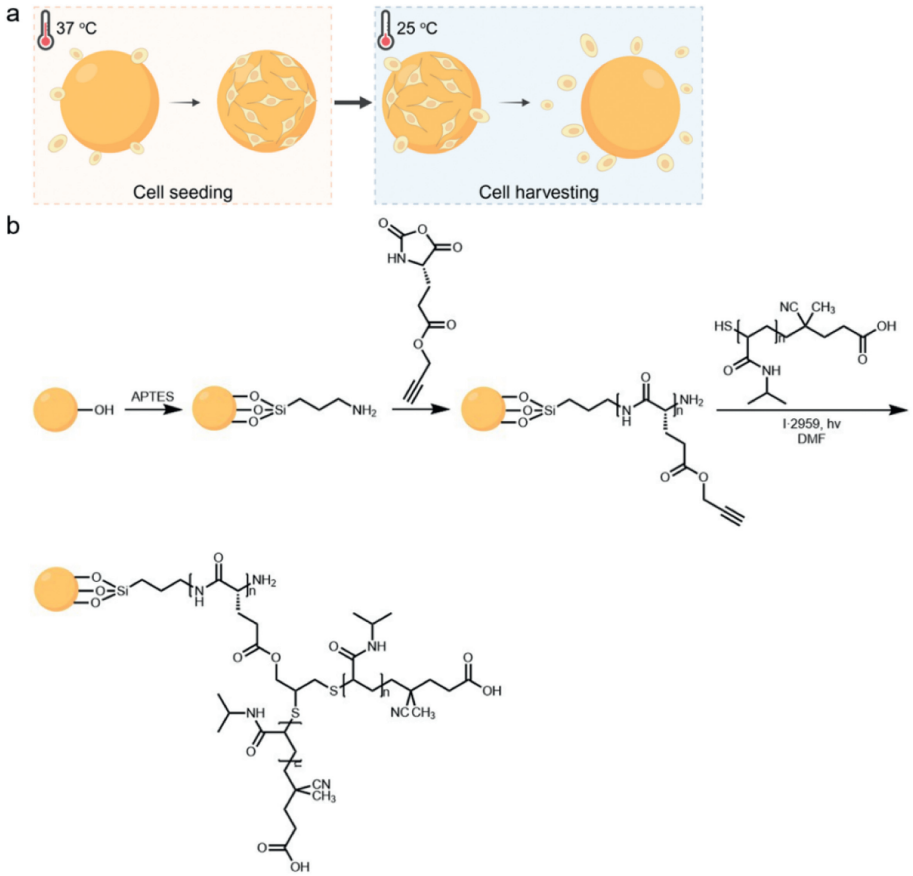

Fig. 1. Schematic illustration of Glass-PPLG-*g*-PNIPAM for cell cultivation and enzyme-free cells harvest. (a) Schematic of cell seeding on the microcarriers and thermally-induced harvest. (b) Preparation scheme of Glass-PPLG-*g*-PNIPAM.

Subsequently, we prepared Glass-PPLG-*g*-PNIPAM by employing a thiol-yne click reaction between PPLG and PNIPAM-SH under UV irradiation (Fig. 1b).

In this study, we investigated the impact of molecular weight on the thermoresponsive properties of PNIPAM. The synthesis procedure for PNIPAM-SH was illustrated in Fig. 2a. Initially, PNIPAM macro-CTA was prepared through RAFT polymerization of NIPAM monomer, using 2,2′-azobis(isobutyronitrile) (AIBN) as the initiator and 4-cyano-4-(dodecylsulfanylthiocarbonyl)sulfanylpentanoic acid (CDSP) as the chain transfer agent. Subsequently, *n*-butylamine was added *via* aminolysis to obtain PNIPAM-SH. While maintaining a constant feed ratio of AIBN, the polymers gradually increased in molecular weight with an elevated monomer to CDSP ratio [12]. As shown in Figs. 2b and c, we obtained a series of PNIPAM-SH samples with varying lengths, all exhibiting unimodal and symmetrical GPC (gel permeation chromatography) curves with narrow molecular weight distributions. The chemical structure of PNIPAM-SH was confirmed through ^{1}H NMR. Fig. 2d displayed the signals of the methylene protons of PNIPAM-SH, which appear at 2.81 ppm. For subsequent characterization, we selected $PNIPAM_{14.8k}$-SH as an example. UV–vis spectra of PNIPAM macro-CTA and PNIPAM-SH demonstrated that aminolysis led to the disappearance of the C=S peak at 310 nm (Fig. 2e) [13]. Furthermore, FTIR spectra of PNIPAM-SH revealed a week vibrational band at 2800 cm^{-1}, corresponding to the S-H stretching vibration (Fig. 2f). Collectively, these data indicated that PNIPAM-SH was successfully synthesized.

Next, PNIPAM was grafted onto the surface of glass microspheres through a click reaction between the thiol group of PNIPAM-SH and the alkyne group on Glass-PPLG. Glass-PPLG was prepared through PLG-NCA ring-opening polymerization. Briefly, γ-propargyl-L-glutamate (PLG) was synthesized by modifying L-glutamic acid with propargyl alcohol. PLG-NCA was synthesized from PLG and triphosgene [14]. As shown in Figs. S1 and S2 (Supporting information), the structure of PLG and PLG-NCA were confirmed by ^{1}H NMR. Glass-PPLG-*g*-PNIPAM was prepared through the thiol-yne click reaction of PNIPAM-SH and Glass-PPLG. Taking Glass-PPLG-*g*-$PNIPAM_{14.8k}$ as an example, the morphologies of Glass, Glass-PPLG and Glass-PPLG-*g*-$PNIPAM_{14.8k}$ microcarriers were examined by SEM, and all exhibited a rounded morphology (Fig. 3a). However, after PNIPAM grafting, Glass-PPLG-*g*-$PNIPAM_{14.8k}$ showed a rougher surface, while unmodified Glass surface remained smooth. The binding of PNIPAM-SH to Glass-PPLG was assessed by examining the S 2p signal. XPS results (Fig. 3b) revealed a distinct S 2p peak at 164 eV, confirming the successful conjugation of PNIPAM-SH onto the surface of the microcarriers. The presence of PNIPAM was further confirmed by EDS mapping. In Fig. 3c and Fig. S3 (Supporting information), it was evident that the content of S and N elements on the surface of Glass-PPLG-*g*-PNIPAM increased, and the uniform distribution of PPLG-*g*-PNIPAM was observed. These findings collectively indicated the successful preparation of Glass-PPLG-*g*-PNIPAM.

The prepared microcarriers was sterilized by autoclaving for subsequent cellular experiments. B16F10 cells were seeded onto the microcarriers. Over a period of 5 days, the cells proliferated on the microcarriers, and cell viability was assessed using CCK-8 assay. As depicted in Fig. 4a, the proliferation rate of B16F10 cells on thermoresponsive microcarriers was approximately 1.08 times higher than that observed in 2D culture on day 5. No significant difference was noted between thermoresponsive microcarriers at all time points. The cell proliferation rate results are based on comparison with 2D culture. On day 1, the surfaces of the microcarriers

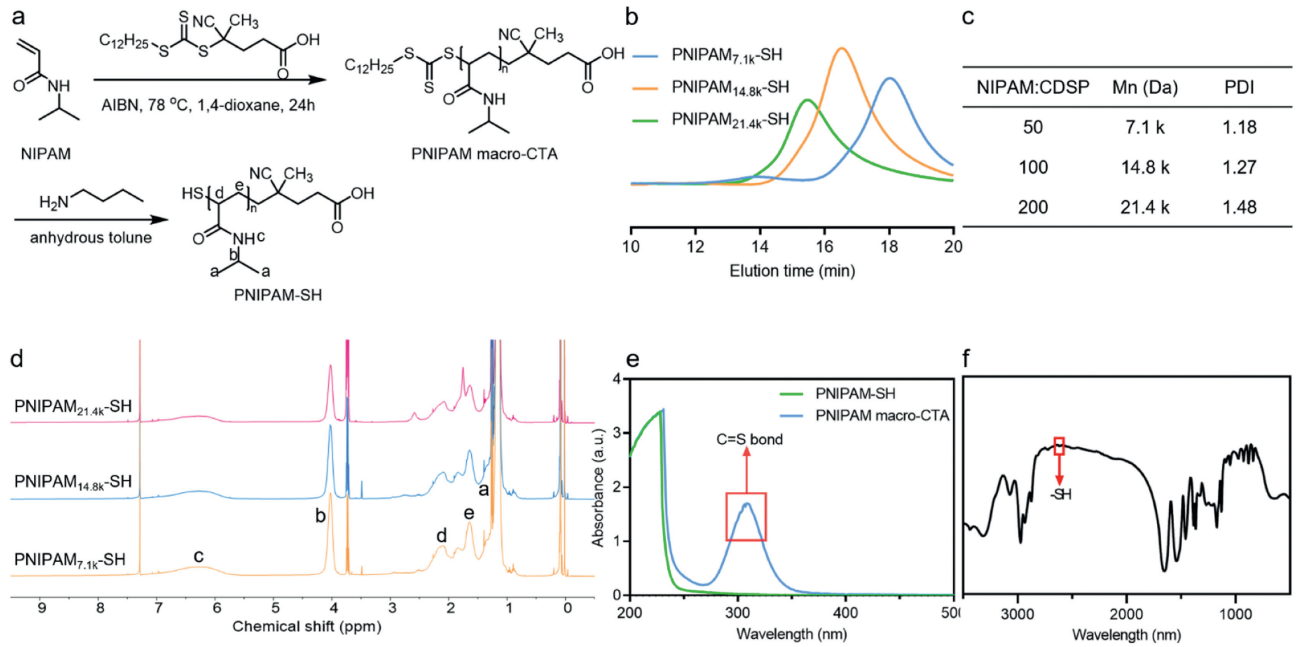

Fig. 2. Analytical confirmation of PNIPAM-SH. (a) Synthetic route of PNIPAM macro-CTA and PNIPAM-SH. (b, c) GPC analysis of PNIPAM-SH. (d) ^{1}H NMR (300 MHz) spectra of PNIPAM-SH in $CDCl_3$. (e) UV–vis absorption spectra of PNIPAM macro-CTA and PNIPAM-SH. (f) FT-IR spectra of PNIPAM-SH.

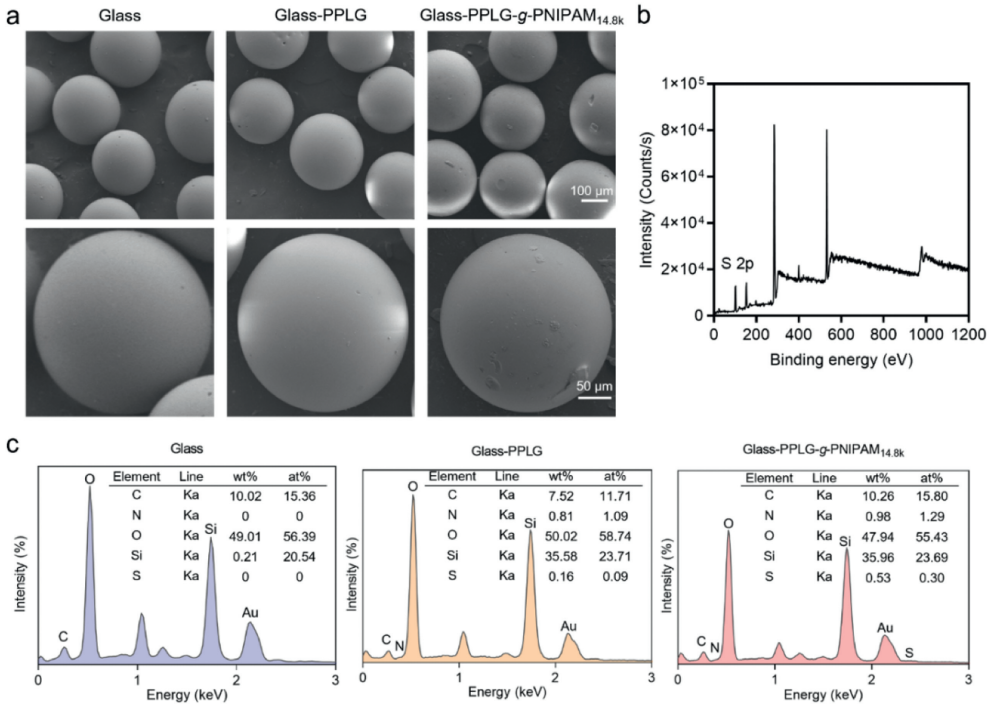

Fig. 3. Characterization of Glass-PPLG-*g*-PNIPAM. (a) SEM images of Glass, Glass-PPLG and Glass-PPLG-*g*-PNIPAM$_{14.8k}$. (b) XPS high-resolution S 2p spectra of Glass-PPLG-*g*-PNIPAM$_{14.8k}$. (c) EDS elemental mapping of Glass, Glass-PPLG and Glass-PPLG-*g*-PNIPAM$_{14.8k}$.

were treated to enhance cell attachment, whereas cells in 2D culture had not fully adhered to the dish at the initial stage which caused cells under the lag phase. Thus, the cell proliferation rate of microcarriers surpassed that of 2D culture. However, on day 3, cells in the 2D culture entered the logarithmic growth phase, leading to higher values than microcarrier culture. On day 5, the cells attached on the surface of microcarriers were still remained in the logarithmic growth phase due to the higher specific surface area-to-volume ratio of microcarriers, resulting in their proliferation rates exceeded that of 2D culture. In addition, the amino groups on the surface of Glass-NH_2 provide positive charge, which promoting cell attachment [15], which caused the highest cell proliferation rate among them on the first day. SEM images (Fig. 4b) depicted the morphology of B16F10 cells cultured on Glass-PPLG-*g*-PNIPAM$_{14.8k}$ on day 3, showing that B16F10 cells spread well on the surface of microcarriers. Culturing cells on thermoresponsive microcarriers allowed for efficient cell expansion compared to traditional 2D culture. After cells reached confluency, a thermally induced cell detachment assay was achieved by lowering the temperature from 37 °C to room temperature (RT). The number of de-

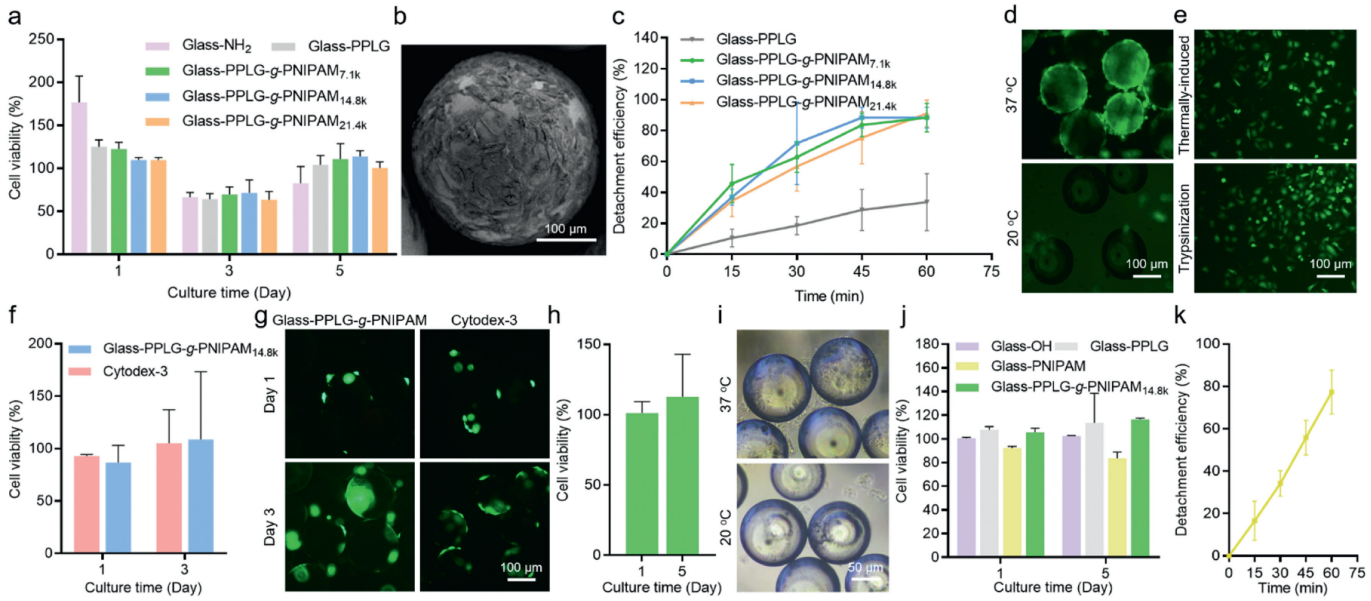

Fig. 4. Cell harvest from the microcarriers and cytocompatibility of microcarriers. (a) The proliferation of B16F10 cells on the surface of microcarriers. (b) SEM image of B16F10 cells cultured on the surface of Glass-PPLG-*g*-PNIPAM$_{14.8k}$ after 3 days incubation. (c) The time-course of temperature-induced B16F10 cells detachment from the surface of microcarriers. (d) Fluorescence microscope images of thermally-induced B16F10-GFP cell detachment at 20 °C for 60 min. (e) Fluorescence microscope images of harvested B16F10-GFP cell recultured in flask for 12 h. (f) The proliferation of B16F10 cells adhered on Glass-PPLG-*g*-PNIPAM$_{14.8k}$ and Cytodex-3. (g) Live/dead fluorescence microscope images of B16F10 cells adhered on Glass-PPLG-*g*-PNIPAM$_{14.8k}$ and Cytodex-3. (h) The proliferation of B16F10 cells adhered on reused Glass-PPLG-*g*-PNIPAM$_{14.8k}$. (i) Optical microscope images of thermally-induced B16F10 cells detachment of reused Glass-PPLG-*g*-PNIPAM$_{14.8k}$ at 20 °C for 30 min. (j) The proliferation of B16F10 cells adhered on Glass-OH, Glass-PPLG, Glass-PNIPAM and Glass-PPLG-*g*-PNIPAM$_{14.8k}$. (k) The time-course of temperature-induced B16F10 cells detachment from the surface of Glass-PNIPAM.

tached cells over time was quantified using a hemocytometer, as shown in Fig. 4c. The percentage of detached cells gradually increased with the increasing incubation time. Compared to microcarriers without grafted PNIPAM, nearly all cells detached from the surface of Glass-PPLG-*g*-PNIPAM within 60 min at RT. This demonstrated that the temperature-dependent hydrophilicity and hydrophobicity transition of PNIPAM allowed cells to detach from the surface without enzymatic treatment. The detachment behavior of B16F10-GFP cells cultured on Glass-PPLG-*g*-PNIPAM$_{14.8k}$ were observed by fluorescence microscope. Fig. 4d showed the microscopic images of B16F10 cells adhered on the microspheres' surface after reducing the temperature to RT. After 60 min incubation at RT, cells almost completely detached from PNIPAM-grafted surface as a cell sheet without using enzymes. To assess the viability of thermally detached cells compared to trypsinization treatment, we recultured detached B16F10-GFP cells and observed them after 12 h. As shown in Fig. 4e, almost all cells have anchored on the flask and exhibited healthy cellular morphology. The experiments on cell detachment rate and biocompatibility using temperature-sensitive microcarriers grafted with different molecular weights of PNIPAM reveal no significant relationship, suggesting that the molecular chain length of PNIPAM have no significant impact on cell detachment due to changes in surface hydrophilicity of microcarriers, nor does it affect cell growth and viability. We further compared the biocompatibility of Glass-PPLG-*g*-PNIPAM and commercial microcarriers, so we selected Glass-PPLG-*g*-PNIPAM$_{14.8k}$ and Cytodex-3 for investigation. Cytodex-3 was a type of microcarriers coated with a layer of denatured collagen, which had been widely used as a substrate for various type of mammalian cells culture [16]. After 1 and 3 days of incubation, as shown in Fig. 4f, both microcarriers exhibited excellent biocompatibility at all time points. The live/dead fluorescence images of Glass-PPLG-*g*-PNIPAM$_{14.8k}$ and Cytodex-3 (Fig. 4g) revealed that cells adhered on the surface and most cells were alive (green), further demonstrating the biocompatibility of Glass-PPLG-*g*-PNIPAM microcarriers for cell attachment, spreading, and proliferation. We next explored the reusability of used microcarriers by washing and re-autoclaving them for subsequent cell culture. As shown in Fig. 4h, the results of cell proliferation experiments showed that the microcarriers were still biocompatible and could achieve cell expansion. As shown in Fig. 4i, cell detachment on the surface of microcarriers was observed after placing them at room temperature for 30 min. These experiments successfully demonstrated the reusability of the prepared microcarriers. To further illustrate the importance of grafted PPLG in microcarrier cell culture, we prepared Glass-PNIPAM by ATRP method. As shown in Figs. S4 and S5 (Supporting information), XPS and EDS results validated its successful preparation. As shown in Fig. 4j, co-incubating B16F10 cells with Glass-OH, Glass-PPLG, Glass-PNIPAM and Glass-PPLG-*g*-PNIPAM$_{14.8k}$, the cell proliferation ability of Glass-PNIPAM was the lowest. As shown in Fig. S6 (Supporting information), the live/dead fluorescence images of Glass-PNIPAM on day 1 also indicated that the viability of cells attached on the surface is not good. Due to PNIPAM lacks the ability to promote cells growth, the proliferation rates of cells attached on Glass-PNIPAM was inferior to those in 2D culture. Compared with Glass-PNIPAM, the cell viability of Glass-PPLG-*g*-PNIPAM$_{14.8k}$ enhanced after modified with PPLG, which underscores the importance of PPLG in microcarrier cell culture environment. PPLG facilitates cell attachment and growth due to the presence of glutamate repeating units. Glass-PNIPAM can achieve temperature-sensitive cell detachment through lowering cultivation temperature. As shown in Fig. 4k, the kinetic curve of cell detachment of Glass-PNIPAM indicated that 77.3% cells detached from the surface of Glass-PNIPAM at 60 min, which is comparable to Glass-PPLG-*g*-PNIPAM$_{14.8k}$.

In conclusion, our study introduced thermoresponsive PNIPAM-grafted glass microcarriers with excellent biocompatibility. By lowering the temperature from 37 °C to RT, these microcarriers achieved a remarkable 90% cell detachment within just one hour, all while maintaining cell viability. This approach ensures the availability of a sufficient number of viable cells for large-scale production. When compared to traditional two-dimensional cell culture, this method has demonstrated its potential for substantial cell expansion, effectively addressing a critical challenge in the broader utilization of cells for various applications.

Declaration of competing interest

The authors declare that they have no known competing financial interests or personal relationships that could have appeared to influence the work reported in this paper.

Acknowledgments

This work was supported by the name of National Key Research and Development Program of China (No. 2021YFB3800900), the National Natural Science Foundation of China (Nos. 51925305, 51873208, 1833010, 51973217, 52373161) and Jilin Province Science and Technology Development Program (No. 20200201075JC).

Supplementary materials

Supplementary material associated with this article can be found, in the online version, at doi:10.1016/j.cclet.2024.109549.

References

[1] N. Chaicharoenaudomrung, P. Kunhorm, P. Noisa, World J. Stem Cells 11 (2019) 1065–1083.
[2] R. AlKhatib, A. Hilal-Alnaqbi, M. Naciri, et al., Front. Biosci. 9 (2017) 172–179.
[3] H. Tavassoli, S.N. Alhosseini, A. Tay, et al., Biomaterials 181 (2018) 333–346.
[4] R. Alfred, J. Radford, J. Fan, et al., Biotechnol. Prog. 27 (2011) 811–823.
[5] B. Koh, N. Sulaiman, M.B. Fauzi, et al., Cell Biosci. 10 (2020) 75.
[6] T.W. Gilbert, T.L. Sellaro, S.F. Badylak, Biomaterials 27 (2006) 3675–3683.
[7] T. Okano, N. Yamada, H. Sakai, Y. Sakurai, J. Biomed. Mater. Res. 27 (1993) 1243–1251.
[8] L. Hou, P. Wu, Soft Matter 10 (2014) 3578–3586.
[9] S.M.H. Dabiri, E. Samiei, S. Shojaei, et al., Small 17 (2021) 2103192.
[10] J.E. Chung, M. Yokoyama, T. Aoyagi, et al., J. Control. Release 53 (1998) 119–130.
[11] A. Tamura, M. Nishi, J. Kobayashi, et al., Biomacromolecules 13 (2012) 1765–1773.
[12] S. Liu, S. Wu, Q. Chen, ACS Macro Lett. 9 (2020) 917–923.
[13] K. Kusolkamabot, P. Sae-ung, N. Niamnont, et al., Langmuir 29 (2013) 12317–12327.
[14] C. Xiao, C. Zhao, P. He, et al., Macromol. Rapid Commun. 31 (2010) 991–997.
[15] S. Derakhti, S.H. Safiabadi-Tali, G. Amoabediny, M. Sheikhpour, Mater. Sci. Eng. C 103 (2019) 109782.
[16] C.F.J. Kuo, C.J. Mei, C.C. Huang, et al., Eur. Polym. J. 195 (2023) 112238.